

A Kinetic Model of a Cyclic System for the Fluorometric Microdetermination of Adenosine Triphosphatase Activity

WILLIAM M. HART, JR.

Department of Physiology, University of Maryland School of Medicine, Baltimore, Maryland 21201

(Received July 30, 1969)

SUMMARY

The derivation of a series of kinetic rate equations to model a cyclic, multistep, fluorometric assay for ADP-generating systems is described. The reaction curves predicted by the model equations are compared with experimentally observed velocities for ATPase reactions to show that reaction rates that are constant and rate-limited by the rate of ADP generation are easily obtained within practical limits of auxiliary enzyme concentrations. The potential of this technique for the study of substrate-enzyme interactions over wide ranges of substrate and enzyme concentrations is discussed.

INTRODUCTION

Cycling or regenerating enzyme systems have been developed for the quantitative microdetermination of a wide variety of substrates (1), and the kinetic behavior of such systems has been well described. Cha and Cha (2) considered such systems, taking into account the depletion of free substrate by binding with relatively high enzyme concentrations. With few exceptions, however (3), cycling techniques have not been considered practical or necessary for the quantitative study of enzyme activities. Bergmeyer (4) has shown, for example, that

This work is being submitted by the author in partial completion of the requirements for the doctoral degree at the University of Maryland Graduate School. Support was provided by United States Public Health Service Grant AM6159. Computer time for this project was made available in part through the facilities of the Computer Science Center of the University of Maryland, College Park.

for the accurate study of myokinase activity, using a spectrophotometric, coupled-reaction technique, the necessarily high quantities of auxiliary enzymes can be impractical. By using a photoelectric fluorometer in the measurement of the indicator substrate in such a system (DPNH), the entire range of magnitudes of substrate and enzyme concentrations can be adjusted within practical limits so that convenient, accurate microdetermination of enzyme activities becomes possible. Furthermore, by using kinetic models such as the one developed below, one can predict the feasibility and general behavior of a given system prior to its experimental use. Advantages inherent in the use of such systems include, besides the ability to work with micro-sized quantities of sample, a built-in means of stabilizing substrate concentrations at any chosen level so that constant "initial velocities" are observed. In this way substrate-enzyme interactions at very low substrate (or high en-

zyme) concentrations can be accurately studied.

MATERIALS AND METHODS

Adenosine diphosphate, phosphoenolpyruvate (tricyclohexylammonium salt), and bovine serum albumin were purchased from Calbiochem. DPNH and pyruvate kinase were purchased from Boehringer, and lactate dehydrogenase from Worthington. The magnesium salt of adenosine triphosphate was obtained from Sigma Chemical Company. The enzymes were crystalline suspensions in ammonium sulfate solution and were centrifuged just prior to use, the supernatant fluid being removed and the enzyme dissolved in 0.02% bovine serum albumin solution buffered with 0.05 M imidazole HCl to an appropriate pH.

Oxidation of DPNH was followed continuously in a Farrand photoelectric fluorometer, model A₃, equipped with a Corning No. 5840 primary filter and No. 3387 and No. 4308 secondary filters, output signal being read on a microammeter. Stable reading levels were maintained by repeated comparison with arbitrary quinine sulfate standards. Calibration of the fluorescence scale was obtained by addition of a spectrophotometrically standardized ADP solution to the assay system. Reactions were initiated by addition of 1 μ l of sample to a 1-ml reaction tube containing 0.5 mM phosphoenolpyruvate, 0.015 mM DPNH, 3.0 mM Mg ATP, 20 mM KCl, 0.02% bovine serum albumin, and sufficient quantities (approximately 0.5 unit/ml) of the crystalline enzymes. The pH was buffered by 0.05 M imidazole HCl at 7.4. Experimental and

theoretical data were processed in a large, time-sharing digital computer, and results were displayed by way of an automated *x-y* plotting device (California Computer Products, Inc.).

DERIVATION AND SOLUTION OF MODEL EQUATIONS AND DISCUSSION OF RESULTS

The model, as derived here, is based on the scheme shown in Fig. 1. As will be seen, however, in its fully developed state the model is generally applicable to a variety of similar systems. The first series of equations is based on the most stringent level of simplifying assumptions: (a) that the first step (ATP hydrolysis) is a zero-order rate, (b) that the second (kinase) step is pseudo-first-order, i.e., the condition phosphoenolpyruvate \gg ADP holds throughout the period of assay, and (c) that the third step also obeys pseudo-first-order kinetics (DPNH \gg pyruvate). Given these assumptions, the rate of change of ATP concentration is given by¹

$$\frac{d\text{ATP}}{dt} = k_2 \text{ADP} - v \quad (1)$$

where v is the zero-order velocity of hydrolysis and k_2 is the first-order rate constant of the kinase step. Since at any time $\text{ATP} + \text{ADP} = K$, where K is some initially chosen constant, it follows that

$$\frac{d\text{ADP}}{dt} = -\frac{d\text{ATP}}{dt} \quad (2)$$

Substitution of Eq. 2 into Eq. 1 and integrating yields

$$\text{ADP} = \frac{v}{k_2} (1 - e^{-k_2 t}) \quad (3)$$

With the assumption of first-order kinetics for the kinase and the dehydrogenase steps,

¹ In all rate equations the use of brackets to designate molar concentrations has been omitted. Dependent (substrate) variables will have the units of concentration (millimoles per liter), and rates will have the units of concentration per time (millimoles per liter per minute).

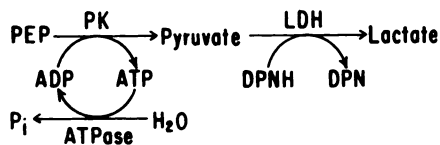


FIG. 1. Reaction scheme of ATPase assay system

PEP, phosphoenolpyruvate; PK, pyruvate kinase; LDH, lactate dehydrogenase.

it follows that the rate of change of pyruvate² concentration is given by

$$\frac{d\text{Pyr}}{dt} = k_2 \text{ADP} - k_3 \text{Pyr} \quad (4)$$

where k_3 is, similarly, the first-order rate constant for the dehydrogenase. Substitution of the value for ADP in Eq. 3 into Eq. 4 and integrating yields

$$\text{Pyr} = v \left[\frac{1}{k_3} (1 - e^{-k_3 t}) - \frac{1}{k_3 - k_2} (e^{-k_2 t} - e^{-k_3 t}) \right] \quad (5)$$

Finally, the rate of DPNH oxidation is given by

$$\frac{d\text{DPNH}}{dt} = -k_3 \text{Pyr} \quad (6)$$

A similar substitution of the expression defining pyruvate, given by Eq. 5, into Eq. 6, and integrating, gives

$$\begin{aligned} \text{DPNH} = & \text{DPNH}_0 \\ & + v \left\{ \frac{1}{k_3} (1 - e^{-k_3 t}) - t + \frac{k_3}{k_3 - k_2} \right. \\ & \left. \cdot \left[\frac{1}{k_3} (e^{-k_3 t} - 1) - \frac{1}{k_2} (e^{-k_2 t} - 1) \right] \right\} \quad (7) \end{aligned}$$

where DPNH_0 is the concentration of DPNH at zero time.

The theoretical data predicted by these equations were generated in a digital computer for a series of magnitudes of the constants v , k_2 , and k_3 . The results for Eq. 3 (predicting ADP concentrations) and for the equation

$$\text{ATP} = \text{ATP}_0 - \text{ADP}$$

where ATP_0 is the initial concentration of ATP, are shown in Fig. 2 for various values of the ratio k_2/v . As can be seen, assuming initial concentrations of zero for ADP and 1.0 mM for ATP, and with a zero-order velocity of ATP hydrolysis of 0.0015 mmole/liter/min (close to the maximal velocities

² The abbreviations used in the equations are: Pyr, pyruvate; PEP, phosphoenolpyruvate.

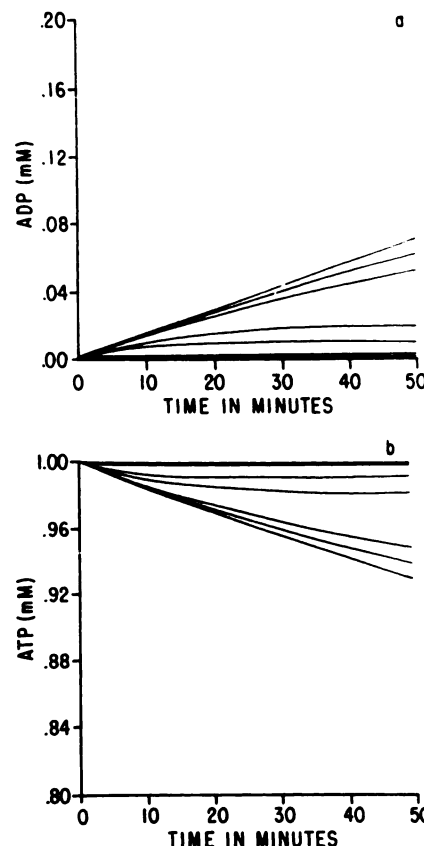


FIG. 2. The data predicted by Eq. 3(a) and by $\text{ATP} = \text{ATP}_0 - \text{ADP}$ (b)

Initial conditions were: $v = 0.0015$ mmole/liter/min, $\text{ATP}_0 = 1.0$ mmole/liter, and k_2 is given seven different values representing the seven lines in each of the graphs. These values are 1, 5, 10, 50, 100, 500, and 1000 times the value of v . The lowest magnitudes of k_2 produce the greatest deflections of curves in both graphs.

encountered in the experimental situation), by choosing values for the ratio k_2/v that are sufficiently high (500–1000) the ATP concentration can be made to remain essentially constant and not significantly different from its initial concentration. Conversely, ADP concentrations under the same conditions are kept very low. Where $k_2/v = 1000$, ADP concentration rises quickly to a plateau at 1 μM , while ATP is maintained at 1.0 mM, only 0.1% of the cycling pair being permitted to exist as ADP.

The data predicted by Eq. 5 and 7 are

shown in Fig. 3. Each graph represents a single value for k_2/v , and each graph contains seven lines representing varying values for the ratio k_3/k_2 . The values for the latter

ratio are 1, 5, 10, 50, 100, 500, and 1000. The lowest values for the ratio k_3/k_2 give the greatest scale deflections in pyruvate concentration and the slowest rates of

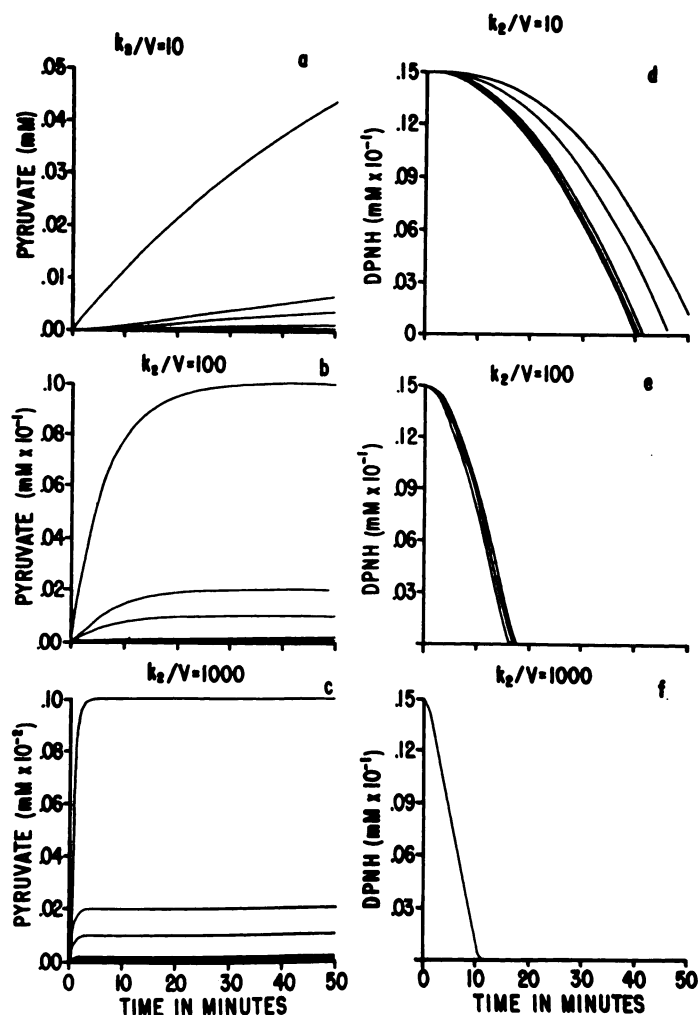


FIG. 3. The curves predicted by Eq. 5 (a-c) and those predicted by Eq. 7 (d-f)

All abscissae are identical. Each graph represents a different value of the ratio k_2/v , indicated by the figures in the upper part of each graph, and each graph contains seven lines representing the seven values (1, 5, 10, 50, 100, 500, and 1000) of the ratio k_3/k_2 . The lowest values of the latter ratio produce the greatest curve deflections in a-c, and the slowest rates of fall (deflections) in d-f. Notice that as the values of the ratios of the rate constants increase, the predicted curves fall closer to one another, so that in a-c the ordinate scale values producing full-scale deflections of the lowest ratio (k_3/k_2) curves give curves for the higher ratios that are indistinguishable from the abscissa. Similarly, in d, increases in the value of k_3/k_2 produce a family of curves that become progressively indistinguishable from one another, and as k_2/v increases to 1000 (in f) this effect reaches a maximum, with all seven curves being essentially identical. Initial conditions were: $v = 0.0015$ mmole/liter/min, k_2 and k_3 as described above, and $\text{DPNH}_0 = 0.015$ mmole/liter. The symbol V in the figure corresponds to the zero-order velocity, v , used in the text.

DPNH oxidation. It is readily evident that as k_2/v increases, the slopes of the pyruvate curves change from those which rise continuously with time to those which rise rapidly to stable plateaus at low concentrations. Thus, when $k_2/v = 1000$ and $k_3 = k_2$, pyruvate achieves a steady-state plateau concentration of 10^{-3} mM within 4 min of zero time. The DPNH oxidation curves, which represent the curves to be observed experimentally, show that as k_2/v increases to 1000, the curves are transformed from those showing significant lag periods to the final state, where nearly perfect linearity is achieved. Here the slope of the oxidation curves is numerically equal to the rate v of ATP hydrolysis. Of equal interest in this situation is the fact that the seven lines have merged into a single, indistinguishable pattern, meaning that when k_2/v is sufficiently large, k_3 need be only as great as or greater than k_2 to give linear reaction curves that are rate-limited by v .

Since, when k_2/v is sufficiently large, ATP concentration does not vary significantly from its original level, it can be assumed that, regardless of the actual order of the hydrolysis reaction, it will always behave as if it were zero-order (constant velocity). Therefore, the curves predicted by the equations derived following the assumption of first-order kinetics for the hydrolysis reaction should give similar results. In the next series of equations the simplifying assumptions will be that all steps of the system obey first- or pseudo-first-order kinetics. The equation for the rate of change of ADP concentration following the first-order assumption is

$$\frac{d\text{ADP}}{dt} = k_1(\text{ATP}_0 - \text{ADP}) - k_2\text{ADP} \quad (8)$$

where ATP_0 is the initial concentration of ATP and k_1 is the first-order rate constant of the hydrolysis reaction. Integration of Eq. 8 gives

$$\text{ADP} = \frac{k_1}{k_1 + k_2} \text{ATP}_0 (1 - e^{-(k_1+k_2)t}) \quad (9)$$

Methods similar to those used for the derivation of Eq. 5 and 7 yield the following equations for pyruvate and DPNH, following the first-order assumption for the hydrolysis reaction.

$$\text{Pyr} = \frac{k_1 k_2 \text{ATP}_0}{k_1 + k_2} \left[\frac{1}{k_3} (1 - e^{-k_3 t}) + \frac{1}{k_1 + k_2 - k_3} (e^{-(k_1+k_2)t} - e^{-k_3 t}) \right] \quad (10)$$

$$\begin{aligned} \text{DPNH} = \text{DPNH}_0 + \frac{k_1 k_2 \text{ATP}_0}{k_1 + k_2} & \cdot \left\{ \frac{1}{k_3} (1 - e^{-k_3 t}) - t \right. \\ & + \frac{k_3}{k_1 + k_2 - k_3} \left[\frac{1}{k_3} (1 - e^{-k_3 t}) \right. \\ & \left. \left. - \frac{1}{k_1 + k_2} (1 - e^{-(k_1+k_2)t}) \right] \right\} \quad (11) \end{aligned}$$

Again k_1 , k_2 , and k_3 are the first-order rate constants of the hydrolysis, kinase, and dehydrogenase steps, respectively, and ATP_0 and DPNH_0 define initial conditions and have the units of concentration.

The data predicted by Eq. 9 and by the equation

$$\text{ATP} = \text{ATP}_0 - \text{ADP}$$

are shown in Fig. 4. As can be seen, the results are nearly identical with the first case shown in Fig. 2. When the value of the ratio k_2/k_1 is sufficiently large (500–1000), a steady state is rapidly attained by the system, which is characterized by a stable plateau concentration of ATP not significantly different from its initial value. Conversely, ADP concentration is not permitted to rise above a level of $0.2 \mu\text{M}$, and less than 0.1% of the cycling pair exists as ADP.

The computer-generated predictions of Eq. 10 and 11 are shown in Fig. 5. As can be seen, when the initial velocity of hydrolysis is again 0.0015 mmole/liter/min ($\text{ATP}_0 = 0.1$ mM, $k_1 = 0.015$), the shape of the DPNH oxidation curves for the case when $k_2/k_1 = 100$ is in every way similar to the situation in which $k_2/v = 1000$ following the

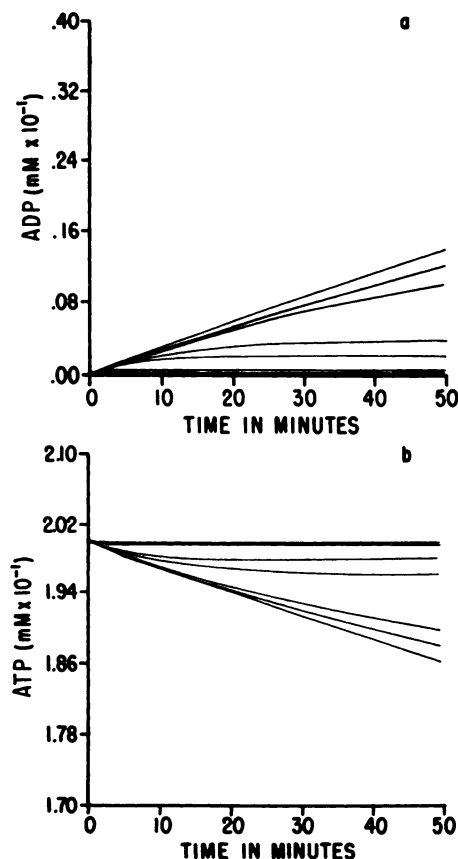


FIG. 4. Data entirely analogous to those of Fig. 2, representing the predictions of Eq. 9(a) and the equation $ATP = ATP_0 - ADP$ (b)

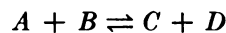
The seven lines in each graph represent the seven values (1, 5, 10, 50, 100, 500, and 1000) of the ratio k_2/k_1 . The lowest values of this ratio produce the greatest curve deflections in both graphs. Initial conditions were: $ADP = \text{zero}$, $ATP_0 = 0.2 \text{ mmole/liter}$, $k_1 = 0.0075/\text{min}$, and k_2 as defined above. Thus, the initial velocity of ATP hydrolysis [$k_1(ATP_0 - ADP)$] is defined as $0.0015 \text{ mmole/liter/min}$ (see the text).

zero-order assumption (Fig. 3). The pyruvate curves predicted by Eq. 10 show typical "lag periods" at low k_2/k_1 ratios, but these become indistinguishable as the ratio increases. Again, if the numerical value of k_2 is 1000 times the initial velocity of hydrolysis, pyruvate concentration rapidly attains plateaus at low levels, and nearly perfect linear oxidation curves are achieved for DPNH for all $k_3 \geq k_2$. Notice that the

magnitude k_2 must have, relative to k_1 , to yield linear oxidation curves is actually independent of the value for the first-step rate constant (k_1) and depends solely on the actual initial rate of hydrolysis ($k_1 \cdot ATP_0$). Therefore, if in the experimental situation k_2 is set at a level 1000 times the highest initial velocity expected, linear curves will be obtained regardless of the order of the hydrolysis reaction. Simply stated, this means that if ATP regeneration, catalyzed by pyruvate kinase, is sufficiently rapid (1000 times as fast as hydrolysis), ATP concentration will not change significantly, and the hydrolysis reaction will behave throughout the period of assay as if it were zero-order (constant velocity).

Evaluation of rate constants as described above is of little help in determining exact quantities of crystalline enzyme preparations needed to catalyze a given assay reaction. For instance, following the assumption of first-order kinetics for a given reaction, the rate constant is expressed in units of time^{-1} . The physical meaning of such units is difficult to interpret. Commercially available enzyme preparations are usually labeled as having a given number of "units" per milligram of protein. The units given are most commonly micromoles of substrate consumed per minute under optimal conditions and saturating levels of substrate. Thus, in adding a given quantity of crystalline enzyme to a reaction, one knows the potential maximal velocity of the reaction catalyzed by the enzyme, expressed in units of concentration per time. To be useful in predicting the quantity of enzyme needed in catalyzing a given reaction, a model should predict maximal velocity. In this way an absolute, rather than a relative, activity level is predicted. Accordingly, a third set of equations is derived for the system, using the least number of simplifying assumptions.

For an enzyme-catalyzed, bimolecular reaction of the form



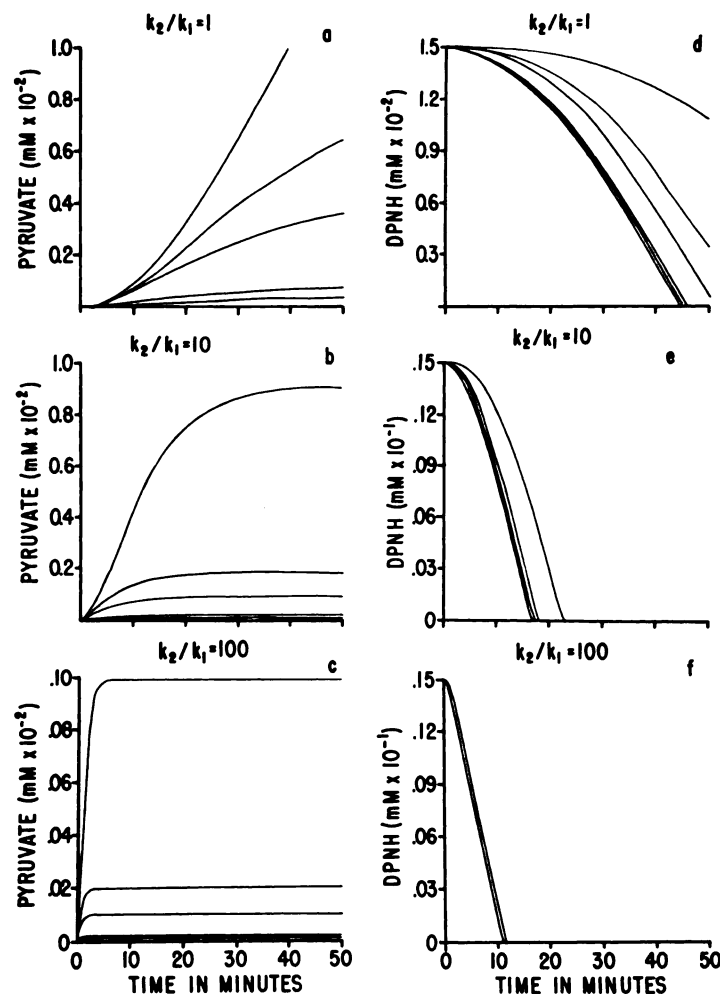


FIG. 5. The curves predicted by Eq. 10 (a-c) and those predicted by Eq. 11 (d-f)

The values of the ratios of rate constants are arranged in a manner precisely analogous to Fig. 3 (see legend to Fig. 3). Initial conditions were: $\text{ATP}_0 = 0.1$ mmole/per liter, $\text{DPNH}_0 = 0.015$ mmole/liter, $k_1 = 0.015/\text{min}$, and k_2 and k_3 as previously defined. Note again that the initial rate of ATP hydrolysis ($k_1 \cdot \text{ATP}_0$) is defined as 0.0015 mmole/liter/min (see the text).

Alberty (5) has shown that, in the special case in which binding of neither substrate is influenced by the presence of the other, the following equation holds.

$$v = \frac{V_{\max}}{1 + \frac{K_m^A}{A} + \frac{K_m^B}{B} + \frac{K_m^{AB}}{A \cdot B}}$$

where the K_m constants are those substrate concentrations giving half-maximal velocity when the other member of the substrate pair is saturating, and the constant K_m^{AB} is a

complex constant approximated by the product of the individual K_m values. Reynard *et al.* (6) have shown that pyruvate kinase behaves experimentally in a manner that conforms to the predictions of the above equation ($K_m^{AB} = K_m^A \times K_m^B$). Similarly, Zewe and Fromm (7) have demonstrated analogous kinetic behavior in lactate dehydrogenase from rabbit muscle.

The final state of the model has been constructed using the above information.

Provided that pyruvate kinase and lactate dehydrogenase obey the predictions of the above equation, and assuming Michaelis kinetics for the ATPase reaction, the rate of change of ATP concentration will be given by

$$\frac{d\text{ATP}}{dt} = \frac{V_2}{1 + \frac{K_m^{\text{ADP}}}{\text{ADP}} + \frac{K_m^{\text{PEP}}}{\text{PEP}} + \frac{K_m^{\text{ADP}} \cdot K_m^{\text{PEP}}}{\text{ADP} \cdot \text{PEP}}} - \frac{V_1}{1 + \frac{K_m^{\text{ATP}}}{\text{ATP}}} \quad (12)$$

where V_2 is the maximal velocity of the kinase reaction and V_1 is the maximal velocity of the hydrolysis reaction. The rest of the model, similarly derived, is as follows.

$$\frac{d\text{ADP}}{dt} = -\frac{d\text{ATP}}{dt} \quad (13)$$

$$\frac{d\text{PEP}}{dt} = -\frac{V_2}{1 + \frac{K_m^{\text{ADP}}}{\text{ADP}} + \frac{K_m^{\text{PEP}}}{\text{PEP}} + \frac{K_m^{\text{ADP}} \cdot K_m^{\text{PEP}}}{\text{ADP} \cdot \text{PEP}}} \quad (14)$$

$$\frac{d\text{Pyr}}{dt} = -\frac{d\text{PEP}}{dt} - \frac{V_3}{1 + \frac{K_m^{\text{Pyr}}}{\text{Pyr}} + \frac{K_m^{\text{DPNH}}}{\text{DPNH}} + \frac{K_m^{\text{Pyr}} \cdot K_m^{\text{DPNH}}}{\text{Pyr} \cdot \text{DPNH}}} \quad (15)$$

$$\frac{d\text{DPNH}}{dt} = -\frac{V_3}{1 + \frac{K_m^{\text{Pyr}}}{\text{Pyr}} + \frac{K_m^{\text{DPNH}}}{\text{DPNH}} + \frac{K_m^{\text{Pyr}} \cdot K_m^{\text{DPNH}}}{\text{Pyr} \cdot \text{DPNH}}} \quad (16)$$

where V_3 is the maximal velocity of the dehydrogenase reaction.

This final set of five first-order, nonlinear, differential equations (Eq. 12-16) has five dependent and one independent variable. Numerical solution of the system was obtained by using a modified, fourth-order Runge-Kutta technique (8). The K_m values are those published by Bergmeyer (4) for the commercially available preparations of pyruvate kinase and lactate dehydrogenase (see Table 1). Results of the solution are shown in Fig. 6 for varying values of V_2 and V_3 . It has been assumed that the initial ATP concentration is equal to the K_m of hydrolysis ($v = V_1/2$) and that the maximal rate for hydrolysis (V_1) is 0.0015 mmole/liter/min. When V_2 is 10 times the initial velocity, and V_3 is in excess, curve *a* is generated. As V_2 increases in value to 1000 times the initial rate of hydrolysis (a V_2 for pyruvate kinase of 1.5 mmole/liter/min), curves *b* and *c* are produced, while V_3 remains at a value of 1.5. Hence, a linear reaction curve which is absolutely dependent on the initial rate of ATP hydrolysis is achieved

TABLE 1

Summary of initial conditions used and results obtained in solution of Eq. 12-16
See Fig. 6 for graphic results.

Curve	Substrate variables					Constants			Maximum velocity obtained (DPNH oxidation)	Ratio of velocity obtained to rate of ATP hydrolysis
	ATP	ADP	PEP ^a	Pyr ^a	DPNH	V_1	V_2	V_3		
	mmole/liter					mmoles/liter/min			mmole/liter/min	%
<i>a</i>	0.1	0	0.5	0	0.015	0.0015	0.015	15.0	0.000549	79.5
<i>b</i>	0.1	0	0.5	0	0.015	0.0015	0.15	1.5	0.000735	98.0
<i>c</i>	0.1	0	0.5	0	0.015	0.0015	1.5	1.5	0.000750	100.0
<i>d</i>	0.1	0.01	0.5	0	0.015	0	1.5	1.5		

$K_m^{\text{ADP}} = 0.36$, $K_m^{\text{PEP}} = 0.086$, $K_m^{\text{Pyr}} = 0.09$, and $K_m^{\text{DPNH}} = 0.005$ mmole/liter [after Bergmeyer (4)].
 $K_m^{\text{ATP}} = 0.1$ mmole/liter (assumed).

^a See Footnote 2.

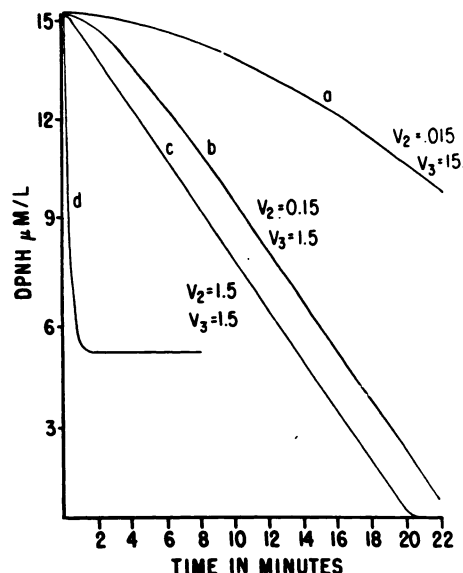


FIG. 6. Curves for the oxidation of DPNH predicted by the simultaneous numerical solution of the system of Eq. 12-16

The initial conditions and values for constants used in the solution are summarized in Table 1. See the text for discussion.

when the absolute activity of pyruvate kinase, measured as units of the crystalline preparation, is equal to about 1000 times the initial rate of hydrolysis, even though the activity of lactate dehydrogenase is of the same order of magnitude. So expressed, V_2 and V_3 represent maximal velocities under ideal conditions and saturating substrate concentration, and it is then a simple matter experimentally to add to an assay system the precise quantities of auxiliary enzymes needed to produce linear curves.

Prior to an assay the system can be tested to confirm that the auxiliary activities are sufficient by adding a known quantity of ADP and measuring the half-time and size of the decay of DPNH. Curve *d* in Fig. 6 shows such a situation predicted by the model in which the ATPase activity (V_1) is presumed to be zero, and the initial concentration of ADP is 10 μM . The decay predicted by the model has a half-time of about 15 sec. Experience has shown that when the half-time of the reaction following addition of ADP is 0.5 min or less, the reac-

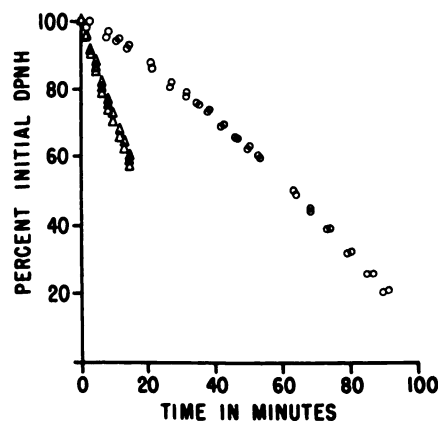


FIG. 7. Results of assay initiated by addition of 1 μl of crude renal homogenate having approximately 0.43 $\mu\text{mole/liter/min}$ of ATPase activity

All reaction tubes contained 3.0 mM MgATP, 0.5 mM phosphoenolpyruvate, 20 mM KCl, 0.015 mM DPNH, and 0.05 M imidazole buffer, pH 7.4, in a final volume of 1 ml. The data indicated by triangles (results of two tubes) show results when the reaction mixture contained 0.5 unit/ml each of pyruvate kinase and lactate dehydrogenase (approximately 1000 times the expected activity of ATPase). The data indicated by circles show results of two determinations when the tubes contained 0.005 unit/ml of pyruvate kinase and 0.5 unit/ml of lactate dehydrogenase (about 1% of the model-predicted optimal concentration of pyruvate kinase). All data have been "normalized" as percentage of initial DPNH concentration.

tion curves obtained during ATPase assay are precisely linear. Initial conditions of substrate variables and values of constants used in the solution of Eq. 12-16 are summarized in Table 1.

Experimental confirmation of the model results is illustrated in Fig. 7. The data points designated by triangles show the results obtained when the reaction mixture contained the model-predicted optimal quantities of auxiliary enzymes for the assay of 1 μl of a crude renal homogenate containing about 0.43 $\mu\text{mole/liter/min}$ of ATPase activity. The data represented by circles in Fig. 7 were obtained under the same conditions with the enzyme pyruvate kinase at about 1% of its predicted optimal concentration. Figure 8 shows examples of experimental data obtained for an ATPase

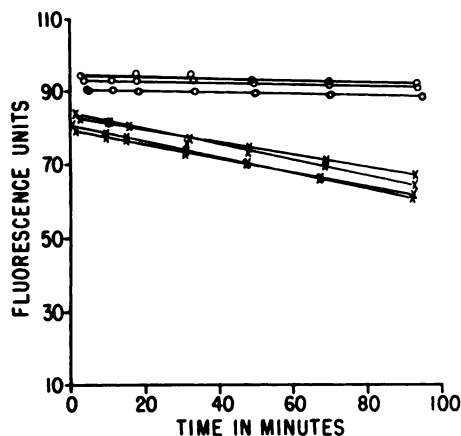


Fig. 8. Actual data from assay of four samples of dilute crude renal homogenate having approximately 15×10^{-3} μ mole/liter/min of ATPase activity for each microliter of sample

Tubes contained the same constituents as previously described, with 0.5 unit/ml each of pyruvate kinase and lactate dehydrogenase. Data indicated by circles are from substrate blanks containing no ATP, while data indicated by crosses are from tubes containing 5.0 mM MgATP. Straight lines, fitted to data points by a least squares method, all have correlation coefficients of 0.995 or better.

assay in which pyruvate kinase and lactate dehydrogenase were present in concentrations of 0.5 unit/ml. The curves were fitted to the points by a least squares method. These data indicate that under routine experimental conditions linear reaction velocities that maintain stability at the

steady state over long and conveniently measured periods of time are easily obtained.

ACKNOWLEDGMENTS

The author wishes to express his gratitude to Dr. John J. O'Neill and Dr. William D. Blake for their invaluable advice and encouragement.

ADDENDUM

McClure (9) has recently dealt with a similar analysis of coupled enzyme assays. Systems involving two auxiliary reactions are dealt with graphically, and a nomogram is provided describing combinations of first-order rate constants required to produce 99% levels of the steady-state concentration of intermediate substrate within given periods of time.

REFERENCES

1. O. H. Lowry, J. V. Passonneau, F. X. Hasselberger and D. W. Schulz, *J. Biol. Chem.* **239**, 18 (1964).
2. S. Cha and C. M. Cha, *Mol. Pharmacol.* **1**, 178 (1965).
3. R. W. Albers, G. J. Koval and G. J. Siegel, *Mol. Pharmacol.* **4**, 324 (1968).
4. H. U. Bergmeyer, "Methods of Enzymatic Analysis," pp. 10, 986, 997. Academic Press, New York, 1965.
5. R. A. Alberty, *J. Amer. Chem. Soc.* **75**, 1928 (1953).
6. A. M. Reynard, L. F. Hass, D. D. Jacobsen and P. D. Boyer, *J. Biol. Chem.* **236**, 2277 (1961).
7. V. Zewe and H. J. Fromm, *J. Biol. Chem.* **237**, 1668 (1962).
8. M. J. Romanelli, in "Mathematical Methods for Digital Computers" (A. Ralston and H. S. Wilf, eds.), p. 110. Wiley, New York, 1960.
9. W. R. McClure, *Biochemistry* **8**, 2782 (1969).